Journal of Geological Resource and Engineering 2 (2014) 39-54

Sensitivity of the CLM 4.0 (Community Land Model Version 4.0) to Key Modeling Parameters and Modeling of Key Physical Processes with Focus on the Arctic Environment

Elena A. Kalinina, William J. Peplinski, Vincent C. Tidwell and David B. Hart

Sandia National Laboratories, Albuquerque 87185, NM, USA

Abstract: The CLM (Community Land Model) simulates major physical processes at the land surface and in the shallow subsurface and calculates the parameters that are then used as the inputs into the atmospheric model. The major goal of this study was to identify the parameters that have greatest impacts on these inputs and thus, the greatest potential to impact the climate in Arctic environment. Another goal was to identify the limitations in representing different physical processes and to determine whether these limitations restrict the ability of CLM to predict the distribution of energy at the land surface. The focus of this analysis is on the vegetation and soil models. The analysis was conducted for a grid cell near Fairbanks, Alaska. A range of hydrogeologic and thermal soil properties and vegetation characteristics was defined for the vegetation and soil parameters. Multiple CLM sensitivity runs were performed. The sensitivity cases that produced noticeable differences either between the mean soil temperatures or/and between ground temperatures were the cases related to the LAI (leaf area index), SAI (stem area index), and soil moisture (shallow water table conditions). These results were explained based on the analysis of the net radiation partitioning at the land surface.

Key words: Soil moisture, soil temperature, vegetation properties, ground heat, latent heat, sensible heat.

1. Introduction

The CLM 4.0 (Community Land Model version 4.0) is the land sub-model of the CESM (Community Earth Systems Model) version 1. CESM is an open-source, FORTRAN language, global climate model maintained by the NCAR (National Center for Atmospheric Research) in Boulder, Colorado. It is the product of on-going development, which started with the CCSM (Community Climate System Model) in 1983. The other modules within the CESM are for atmosphere (Community Atmospheric Model), sea ice (CICE), oceans (Parallel Ocean Program 2), land ice (Glimmer-Community Ice Sheet Model), and the "coupler" which links the modules together.

CLM approximates the land surface using a grid cell approach. A few different resolutions are available. CLM can be run in a stand-alone mode and in a fully coupled mode. The stand-alone mode can model either single cell or multiple cells (regions).

Each grid cell is defined in terms of its land units. The land units are: glacier, wetland, lake, urban, and vegetated. Each land unit is simulated as a one-dimensional column. The vegetated land unit is defined in terms of plant types (this includes bare soil). The vertical profiles of temperature and soil moisture are calculated for each column.

The physical processes simulated by the CLM include the following: absorption, reflection, and transmittance of solar radiation; absorption, reflection, and transmittance of long-wave radiation; momentum, sensible heat, and latent heat; heat transfer in soil and snow; canopy hydrology; snow hydrology; soil hydrology; photosynthesis; lake temperatures and

Corresponding author: Elena Kalinina, Ph.D., research fields: hydrogeology, heat and mass transport modeling, complex systems analysis. E-mail: eakalin@sandia.gov.

fluxes; dust deposition and fluxes; runoff from rivers and oceans; volatile organic compounds; and carbon-nitrogen cycling.

The summary technical description of these models is provided in Ref. [1]. The additional details concerning the specific models and modeling parameters are spread over many different supporting publications and studies. Each model represents a different area or even a discipline and this multi-disciplinary aspect is the major reason of the CLM complexity.

The models in CLM have very different levels of representation of the underlying physical processes. Some models significantly simplify the physical processes. An example is the canopy model in which simple water balance equations are used. The other models use very detail representations of the physical processes. An example is the soil moisture model that implements non-linear modified Richard's equation [1]. However, all the models are inter-related and they either provide the inputs to a downstream model or use the outputs from an upstream model. Due to this, a few iterations are needed to take into account the feedbacks between the models and to make the necessary adjustments in the calculated state variables during each time step.

The diagram in Fig. 1 shows in a simplified form the relationships between the different models. The Sensible Heat, Latent Heat, and Momentum Flux Models are separate and complex models. They are shown in one box because the focus of this analysis was on the hydrogeologic and vegetation models in CLM.

Note that Sensible Heat, Latent Heat, and Momentum Flux Models represent direct interface with the atmospheric model. They use the atmospheric model inputs and they generate the atmospheric model outputs. The vegetation and hydrogeologic models indirectly affect the atmospheric model outputs through their feedbacks to the Sensible Heat, Latent Heat, and Momentum Flux Models. The models with noticeable feedbacks may require detailed physical representation. The goal was to review the vegetation and hydrogeologic models in CLM with this criterion in mind.

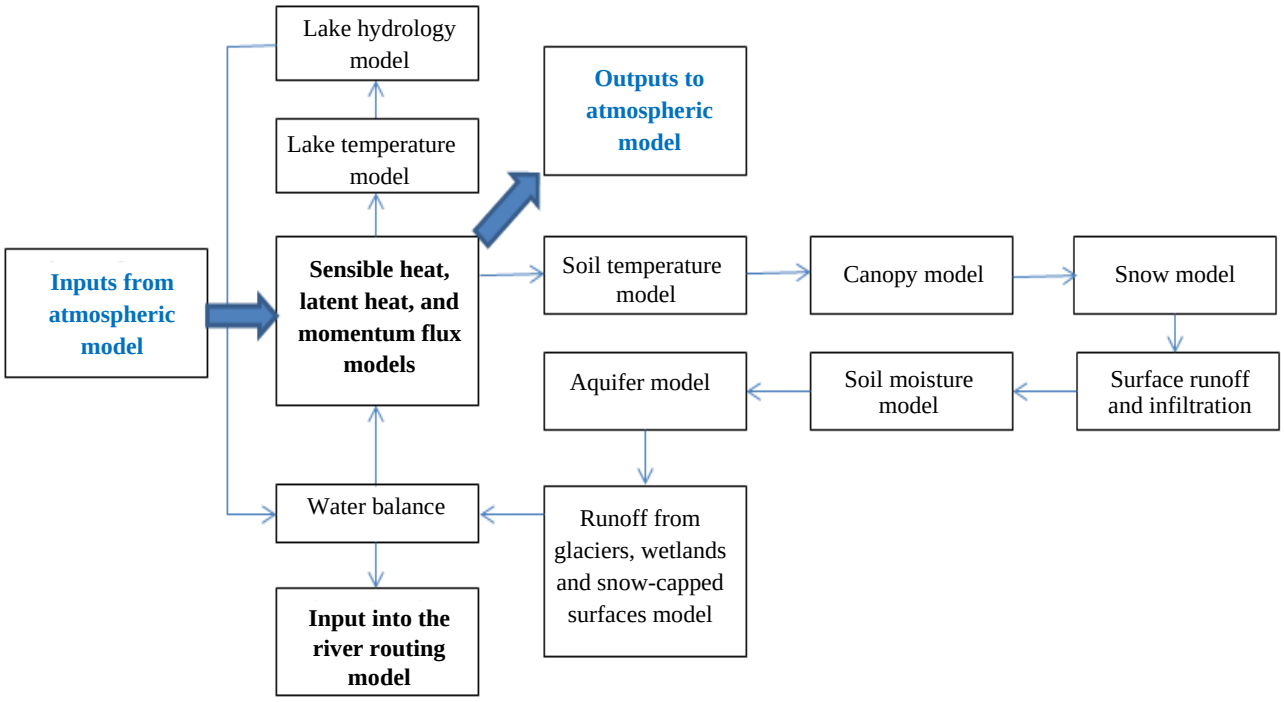

Fig. 1 Simplified diagram of relationships between the CLM models.

2. Materials

The hydrogeologic and vegetation models in CLM have a number of simplifying assumptions. The soil column depth is 3.54 m in any grid cell in the world. The hydraulic and thermal properties of soils are defined based on their organic matter, sand and clay content, which is an approximation that may or may not be applicable at a site-specific scale. The temperature boundary condition at the bottom of the bedrock is zero flux. The aquifer, as implemented in CLM, has infinite resources. This limits the simulations of water withdrawal effects. The subsurface drainage parameters are the same in every grid cell and the rooting depth parameters are fixed for each vegetation type.

The objective was to investigate the potential effects related to some of these assumptions, as well as modeling parameters and physical processes. In order to evaluate the importance of these effects, their impacts on the CLM outputs into the atmospheric model were considered.

The parameters that represent the direct outputs from CLM into the atmospheric model are listed in Table 1. Also considered were the state variables and hydraulic parameters listed in Table 1 because they indirectly affect the outputs into the atmospheric model.

To perform this analysis, CESM and CLM were compiled and run on a high performance computer cluster. CLM was run in the "stand-alone", single grid block mode at a resolution of 0.9 × 1.25 degrees. Because the arctic environment is especially important in the climate studies, we selected a grid block located in the Fairbanks area in Alaska. The scale of a single grid block at that latitude is 62.1 × 36.25 miles. The map of this area is shown in Fig. 2.

A stand-alone CLM run requires an input data set, or forcing data, to take the place of data which would otherwise be provided as output from modules of the CESM. The following parameters are inputs into the CLM: zonal wind, meridional wind, pressure, potential temperature, temperature, specific humidity, incident long-wave radiation, incident diffuse visible radiation, incident diffuse near-infrared radiation, incident direct beam visible radiation, liquid precipitation, solid precipitation, aerosol, and deposition rate.

A historical data set for the CLM, for the period of 1948 to 2004, was compiled by Qian [2]. The atmospheric data are expressed in 3 hour increments,

Table 1 Parameters considered in the sensitivity analysis.

Direct outputs into the atmospheric model	State variables and hydraulic parameters
Latent heat flux (W m^{-2})	Ground heat flux (W m^{-2})
Sensible heat flux (W m^{-2})	Ground temperature (K)
Water vapor flux (mm s^{-1})	Soil temperature in top 10 cm (K)
Zonal momentum flux (kg m^{-1} s^{-2})	Sub-surface runoff (mm s^{-1})
Meridional momentum flux (kg m^{-1} s^{-2})	Surface runoff (mm s^{-1})
Emitted longwave radiation (W m^{-2})	Infiltration (mm s^{-1})
Direct beam visible albedo	Total runoff (mm s^{-1})
Direct beam near-infrared albedo	Aquifer recharge (mm s^{-1})
Diffuse visible albedo	Water table depth (m)
Diffuse near-infrared albedo	Water in unconfined aquifer (mm)
Absorbed solar radiation (W m^{-2})	Soil ice content Soil water content
Radiative temperature (K)	
Temperature at 2 meter height (K)	
Specific humidity at 2 meter height (kg kg^{-1})	
Snow water equivalent (m)	
Aerodynamic resistance (m^{-1})	
Friction velocity (m s^{-1})	

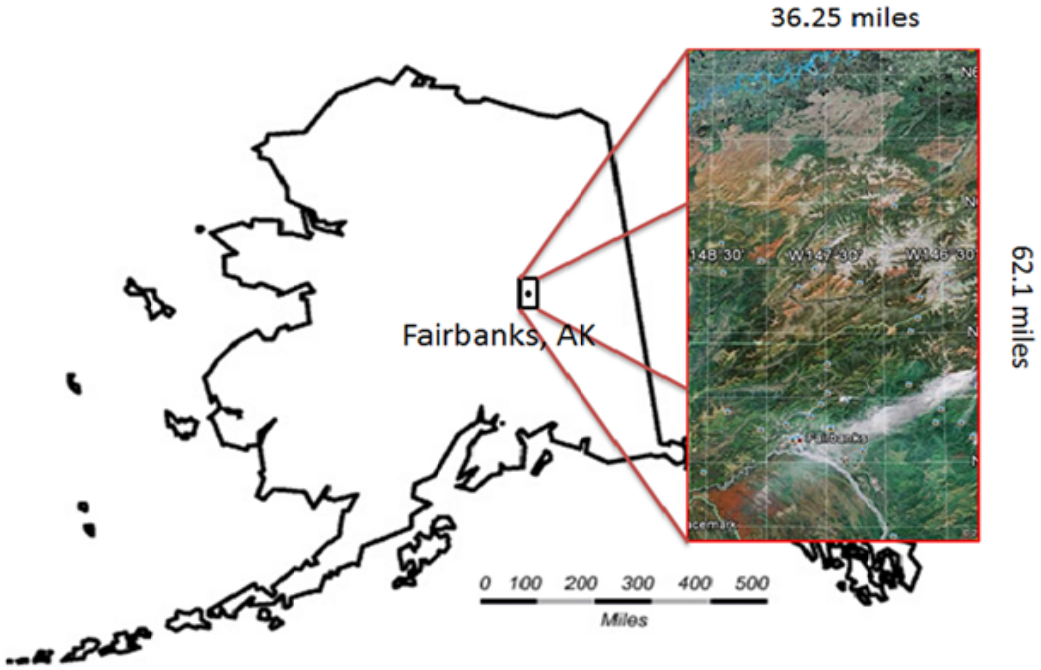

Fig. 2 Fairbanks grid cell.

precipitation in 6 hour increments, and solar data in 6 hour increments. These data were obtained from NCAR and looped through three times in succession to provide necessary inputs for the model runs.

To bring the model to a common starting point a spin-up run for a period of 60 years starting from 1948 was performed. The final state of the model was saved and used as a restart file for all the subsequent runs. After the spin-up run, each of the CLM test runs had a period of 100 years to 150 years. The parameters selected for the sensitivity analysis were the surface data and some hard-wired data as described below.

Each grid cell has the following surface data (resolution is shown in parentheses) associated with it: percent glacier (0.50), percent lake (1.00), percent wetland (0.50), percent urban (1.00), percent sand (5-min), percent clay (5-min), soil organic matter density (1.00), soil color (0.50), maximum fractional saturated area (0.50), percent of vegetated land (0.50), canopy height (top and bottom) (0.50), and monthly leaf and stem area indices (0.50).

CLM reads these input data from the surface data file. A number of other data are “hard-wired” in the code and can be changed only via code modification. The examples are: ground emissivity for soil (0.96); momentum roughness length for soil, glaciers, and wetlands (0.01 m); and heat conductivity of bedrock (3.0 W/m-K).

The Fairbanks grid cell has one land unit, which is vegetated land unit as evident from the map in Fig. 2. The surface data were extracted from the global dataset using regional extraction routine by specifying the coordinates of the grid cell.

The following parameters, including applicable surface data and some hard-wired parameters (last two parameters in the list below), were considered in the sensitivity analysis: soil color, percent sand; percent clay, LAI (leaf area index), SAI (stem area index), canopy bottom and top height, rooting depth, and subsurface drainage.

The applicable variability ranges to be used in the sensitivity analysis were defined for each parameter from this list as described below.

2.1 Soil Color

Soil color affects the dry and saturated soil albedos, which, in turn, impact the energy partitioning at the surface. CLM defines 20 different soil colors, each of

them has saturated and dry visible soil reflectance and saturated and dry near infrared soil reflectance. The soil colors were defined in CLM for each grid cell using a fitting process to get a best match between the albedos calculated by CLM and MODIS satellite observed surface albedos [3].

The soil color in Fairbanks grid cell, as defined in the surface data set, is 18. The potential variation in the soil color was obtained from the map in Ref. [3] showing the world-wide distribution of the soil color classes. According to this map, the variation of soil color in vicinity of Fairbanks area is from 17 to 20, which corresponds to dark low albedo soils. Two cases with the soil color 17 and 20 were considered.

2.2 Soil Texture (Percent Sand and Percent Clay)

Soil texture (percent sand and percent clay) and organic matter density affects thermal and hydraulic properties of soils. These parameters affects the distribution of moisture and temperatures in soil column, ground temperature and surface moisture, which in turns impact the sensible heat, latent heat, and ground heat fluxes. The soil properties in the Fairbank grid cell are listed in Table 2.

As it was discussed earlier, the soil column depth is fixed and is 3.54 m. The soil column is represented with 10 layers with the layer 1 being at the column top. The layer thickness increases exponentially with depth.

There are a number of assumptions associated with the soil models in CLM. The previous CLM versions implemented one set of grid cell specific textural properties for the first 5 top soil layers (depth from 0 to 0.29 m) and second set for the bottom 5 soil layers (depth 0.29 m to 3.63 m). These data were directly prescribed from the global soil profile texture data sets of Reynolds [4]. Originally, these data sets were derived from the FAO/UNESCO (Food and Agriculture Organization /United Nations Educational Scientific and Cultural Organization) Digital Soil Map of the World [5], using the depth and profile methods used by Batjes [6]. Note that FAO/UNESCO data provides information for two soil layers: top soil (depth 0 to 0.30 m) and bottom soil or subsoil (depth 0.30 m to 1.00 m). The bottom soil data were assigned to the CLM soil layer depth 0.29 m to 3.43 m (the lower limit was arbitrarily extended).

In the latest version (CLM4.0) the textural properties (including organic matter density) are prescribed to each of 10 soil layers for each grid point. These more detailed data were derived from the IGBP (International Geosphere-Biosphere Programme) soil data set (Global Soil Data Task, 2000). Note that IGBP data set used the same base data and methods as FAO/UNESCO, Reynolds [4], and Batjes [6], but with the finer resolution.

Five hydrologically inactive ground layers are added to the soil column in order to extend the overall depth to approximately 50 m. These additional layers represent bedrock and are used in the temperature model. Because these layers are hydrologically inactive, the moisture calculations are restricted to the upper 10 layers.

To derive the upper and lower limits for the sand and clay content in the Fairbanks grid cell, the following information was taken into account.

The coefficients of variation of individual soil properties within soils mapped as single series commonly range from 20% to 70%. These coefficients can even be larger when soils are mapped at a higher hierarchical level, such as the FAO soil unit [6].

Table 2 The Fairbanks grid cell soil textural properties.

Layer Number	1	2	3	4	5	6	7	8	9	10
% sand	40	39	39	44	44	48	47	47	49	49
% clay	31	32	32	26	26	25	25	25	27	27
ρ_{om} (kg/m^3)	130	130	130	130	95	61	38	14	0	0

ρ_{om} is the soil organic matter density.

According to the distribution of the textural properties of the top soil in the world-wide soil property map in Lawrence [3], the clay content in the vicinity of the Fairbanks area is from 10% to 30% and the sand contact is from 30% to 60%. Consequently, the clay content in Table 3 is close to its upper limit and the sand content is close to its average value.

Four cases were considered to represent the variability in soil properties: sand content -10%, sand content +10%, clay content -10%, and clay content -20%.

2.3 Vegetation Parameters LAI and SAI

Vegetation parameters affect interception of precipitation and evapotranspiration and thus the distribution of moisture in the soil column and heat and moisture exchange at the ground surface.

Vegetation structure is defined by the LAI, SAI and the canopy bottom and top height. Monthly values of LAI and SAI are defined in CLM for each PFT (plant functional type). LAI is a dimensionless variable defined as one half of the total leaf area per unit ground surface area. SAI is defined as the total area of all the plant stems per unit ground surface area. Monthly LAI values in CLM were developed from the 1-km MODIS-derived monthly grid cell average LAI of Myneni [7]. SAI is calculated from the monthly PFT LAI values using methods of Zeng [8].

There are 3 major vegetation types in the Fairbanks grid cell. These types are: NET (Needleleaf Evergreen Tree) BDS (Broadleaf Deciduous Shrub) Boreal, and Arctic Grass. The area occupied by each PFT expressed as a percent of total vegetated area and the plant specific parameters are presented in Table 3. The monthly LAI and SAI values for the three PFTs are shown in Fig. 3. These data are based on the satellite phenology data for year 2000. The needleleaf forest (NET Boreal) occupies the largest area, has the greatest LAI values and is significantly higher than the other PFTs. Because of this, this PFT was considered in the sensitivity analysis.

The published LAI values for a forest range from 0.4 to 14. The common range for the maximum values is from 6 to 8. To acknowledge this potential variability, two cases shown in Fig. 3 were considered. In the first case, the LAI values are greater by factor of 2. In the second case, the LAI values are smaller by factor of 2. Same principle (factor of 2) was applied to the SAI values.

2.4 Canopy Top and Bottom Height

The canopy top and bottom height affects the plant aerodynamic parameters, which in turn affect the surface fluxes. These parameters are specified for each PFT. The monthly values of all three PFT types present in the Fairbank area are constant. These values are listed in Table 3.

In most of the boreal forests, the dominant trees are needleleaf evergreens—either spruce and fir or spruce and pine. Boreal forests have the simplest structure of all forest formations. They have only one uneven layer of trees. The majority of these tree species are 15 m to 45 m tall. The canopy top height in Table 4 is closer to the lower limit of this range. To take in account this variability, two additional values for the canopy top height were considered—23 m and 30 m. The canopy bottom is defined as one half of the canopy top. This ratio was preserved in the above cases.

2.5 Root Distribution Parameters

The root distribution parameters affect the evapotranspiration and thus the distribution of moisture in the soil column and the heat and moisture exchange

Table 3 PFT characteristics for Fairbanks grid cell.

PFT	% Area	Mean LAI	Mean SAI	Canopy bottom (m)	Canopy top (m)
NET Boreal	60.45	2.426	0.683	8.5	17.0
BDS Boreal	13.5	0.830	0.917	0.1	0.5
Arctic Grass	17	0.838	0.939	0.01	0.5

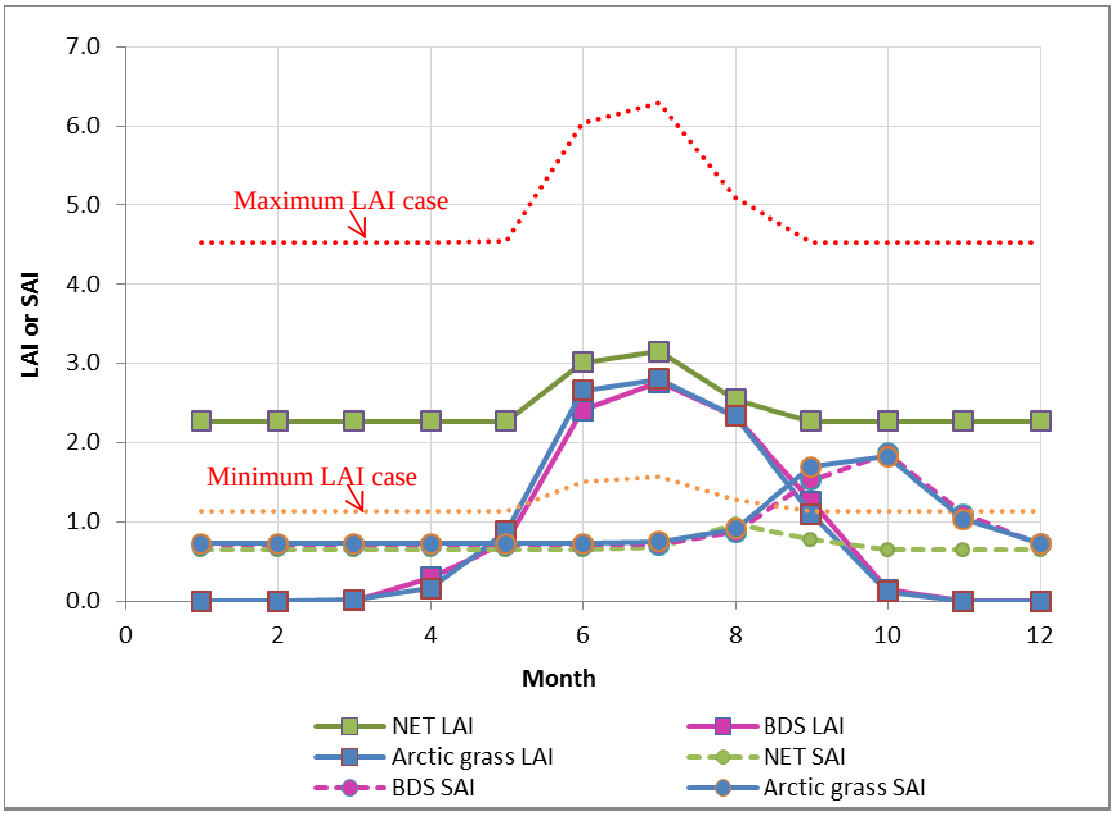

Fig. 3 Monthly LAI and SAI of the dominant PFTs in Fairbanks grid cell.

Table 4 Original and modified cumulative root distribution parameters.

Parameter	Original values	Modified parameter values	
		Deep roots	Shallow roots
Effective rooting depth (m)	1.8	3.54	1
r_a (1/m)	7	10.5	5
r_b (1/m)	2	1.1	4

at the surface.

The cumulative root distribution function (Y) is defined in CLM with two parameters—r_a and r_b. This function is represented in CLM after Zeng [9] as:

$$Y = 1 - 0.5[e^{-r_a d} + e^{-r_b d}] \quad (1)$$

where, d is depth. The effective rooting depth is defined as the depth interval that contains 99 % of roots. The parameters ra and rb are PFT specific. The values of ra and rb for NET Boreal are 7 and 2, respectively. The resulting effective rooting depth is 1.8 m (Fig. 4).

As discussed in Day [10], the shallowest maximum rooting depth of trees is 1 m. The soil depth in CLM is fixed at 3.54 m. Consequently, it is reasonable to assume that the effective rooting depth range from 1 m (shallow roots) to 3.54 m (deep roots). These two cases were considered in the sensitivity analysis.

The values of the parameters r_a and r_b that result in the shallow and deep roots were estimated from Eq. (1). The goal was to find the combination of these parameters that would result in the desirable effective rooting depth while maintaining the same functional shape within the 0 to 50% interval. The resulting parameters are summarized in Table 4. The resulting root distribution functions are shown in Fig. 4

2.6 Subsurface Drainage Parameters

The subsurface drainage controls the moisture conditions in the soil column and the depth to the water table. The subsurface drainage q_{drai} is calculated in CLM

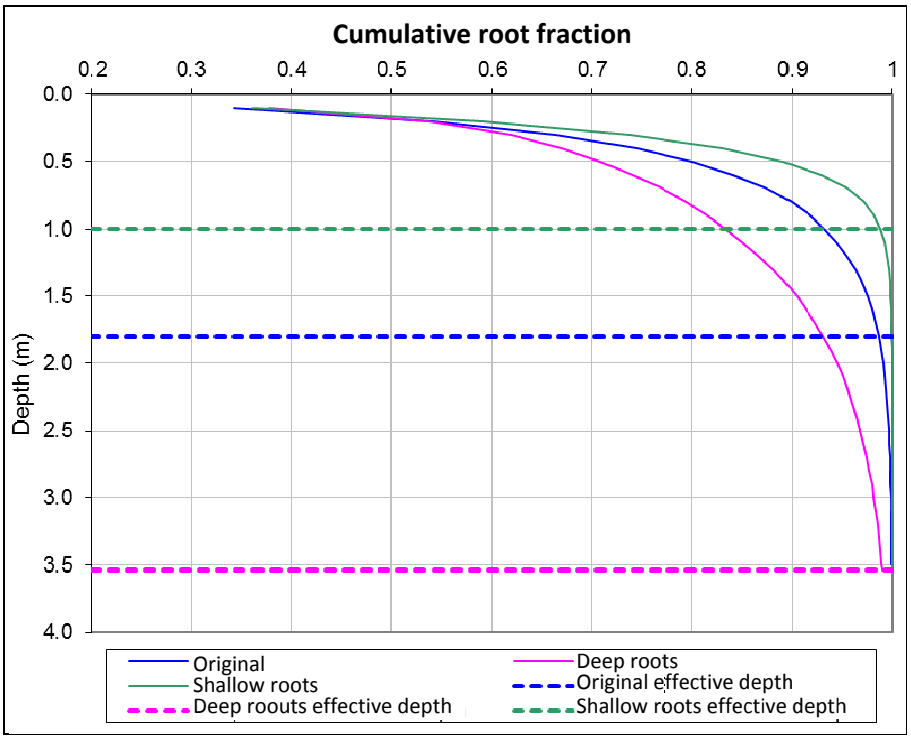

Fig. 4 Original and modified cumulative root distribution functions.

during each time step as:

$$q_{drai} = (1 - f_{imp}) q_{drai,\ max} \exp(-f_{drai} z_\nabla) \quad (2)$$

where, f_{imp} is the impermeable land fraction, f_{drai} is the decay factor, $q_{drai,\ max}$ is the maximum drainage when the water table depth is at the land surface, and z_∇ is the time-dependent depth to water table. The parameters $q_{drai,\ max}$ and f_{drai} are hard-wired in CLM. The respective values are 0.005 kg/m^2-s and 2.5 m^{-1}. These two parameters were determined through the sensitivity analysis and comparison with the observed runoff [1]. They are the same at any location (grid cell) in the world. The subsurface drainage as a function of the water table depth is shown in Fig. 5.

The drainage parameters, as they defined in CLM, result in very small fluctuations of the water table and keep the water table depth around 3 m below the surface, which is at the bottom part of the soil column (Fig. 6). This is because every time when the water table rises, the subsurface drainage increases exponentially, the excess water is quickly removed, and the water table drops. Every time when the water table drops, the drainage stops, and the water table rises. As a result, the shallow water table conditions (saturated soil column) and deep water table conditions (dry soil column) are not effectively represented.

The subsurface drainage parameters were modified as summarized in Table 5. The modified subsurface drainage functions are shown in Fig. 5. The modified parameters allowed for simulating the shallow water table conditions as shown in Fig. 6. Note that the shallow water table conditions are of a special importance because these conditions are common for the artic environment, including the Fairbanks grid cell.

Using the modified drainage function (deep water table case) resulted in the fast drop in the water table to its maximum depth of 80 m (hard-wired in the code). However, this did not dry off the soil column—the changes in the soil moisture were insignificant compared to the original case. To test this condition in a dry and hot climate, we considered a grid cell located in Nevada with the water table located a few hundred meters below the ground. We could not achieve the dry soil profile in this case as well.

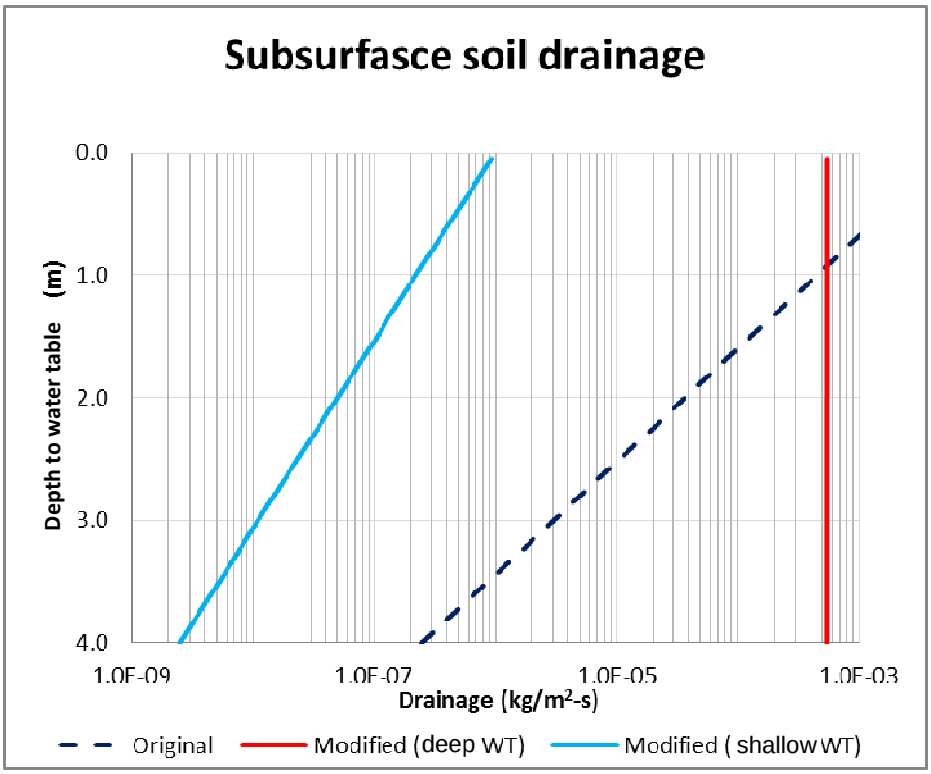

Fig. 5 Subsurface drainage as a function of water table depth with original and modified subsurface drainage parameters.

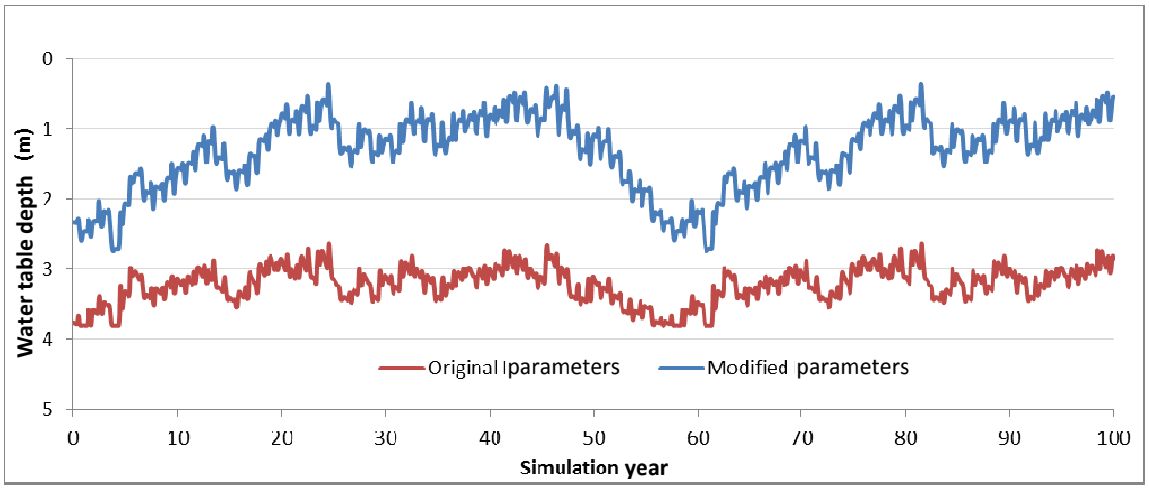

Fig. 6 Water table depth calculated with the original and modified (shallow water table) subsurface drainage parameters.

Table 5 Original and modified subsurface drainage parameters.

Subsurface drainage parameters	Original parameters	Modified parameters	
		Shallow WT	Deep WT
$q_{drai,max}$ (kg/m^2-s)	5.50E-03	1.00E-06	5.50E-04
f_{drai} (1/m)	2.5	1.5	0.001

WT is water table; subsurface drainage parameters are from Eq. (2).

The reason for this was found to be in the way the bottom boundary condition in the soil moisture model is implemented in CLM. While the water table is located within the soil column, the bottom boundary condition is zero flux through the bottom of the soil column. When the water table drops below the soil

column bottom (3.54 m), the low boundary is moved half way between the water table and soil column bottom and fixed pressure and moisture are assigned to it. The fixed pressure and moisture preclude soils from drying off. This boundary condition should be modified to study the effects associated with the dry soils.

3. Results

A stand-alone CLM runs was performed for the base case and for each sensitivity analysis case. The base case in this study is the case with the original surface data extracted for the Fairbanks grid cell and the original rooting depth and subsurface runoff parameters defined in CLM. In each sensitivity case, only one parameter was modified as described above. The output parameters listed in Table 1 obtained for the base case were compared to the corresponding output parameters in the sensitivity analysis cases.

The analysis of these results showed that some output parameters are highly correlated. This provided a basis for reducing parameter number. The direct beam visible albedo, direct beam near-infrared albedo, diffuse visible albedo, and diffuse near-infrared albedo are highly correlated (0.99). Only one of these four parameters was retained for the further analysis. The reference temperature (temperature at the 2 m height) and the ground temperature are highly correlated (0.95) as well. Ground temperature was retained for the further analysis.

The sensitivity cases that produced noticeable differences either between the mean soil temperatures or/and between ground temperatures were the cases related to the following parameters (Table 6):

(1) LAI (both, soil and ground temperature);

(2) SAI (both, soil and ground temperature);

(3) Shallow water table (soil temperature).

The effects of the vegetation and shallow water table on energy constituents are shown in Fig. 7. Soil color, soil texture, canopy bottom and top height, and rooting depth had very little impacts on all the outputs.

The effects of dense vegetation on the ground temperature and soil temperature are shown in Fig. 8. The dense vegetation (LAIx2 case) affects average soil temperature (0.44°C lower than in the base case) and ground temperature (0.50°C lower than in the base case). The drop in temperatures is the result of more heat being reflected from the ground. Lower temperatures lead to greater snow accumulation (larger SWE). The effects of vegetation are significantly greater during the summer time when LAI values are at their maximum values. The ground and soil temperatures are, on average, 0.88°C (ground) and 0.66°C (soil) lower in the summer in the dense vegetation case and on average 0.25°C (ground) and 0.28°C (soil) lower in the winter.

Note that the vegetation parameter LAI (and to lesser extent SAI) has potential to impact the atmospheric model through its effects on the atmospheric temperature (correlated with ground temperature) and the ground heat. The effects due to natural variability considered in this analysis are moderate. However, larger effects might be expected when the vegetation is significantly changed due to either impacts (land management) or catastrophic event (fires).

Table 6 Mean ground and mean soil temperatures in selected sensitivity runs.

Sensitivity case	Mean ground temperature (°C) (% change from the base case)	Mean soil temperature (°C) (% change from the base case)
Base case	-7.87 (NA)	-2.58 (NA)
LAIx2	-8.37 (6.4%)	-3.02 (17.1%)
LAIx0.5	-7.68 (-2.4%)	-2.21 (-14.3%)
SAIx2	-7.94 (0.9%)	-2.36 (-8.5%)
SAIx0.5	-7.84 (-0.4%)	-2.63 (1.9%)
Shallow WT	-7.80 (-0.9%)	-1.51 (-41.5%)
LAIx0.5, SAIx0.5, and shallow WT	-7.80 (-0.9%)	-1.42 (-45.0%)

The selected runs are the ones that produced noticeable changes from the base case.

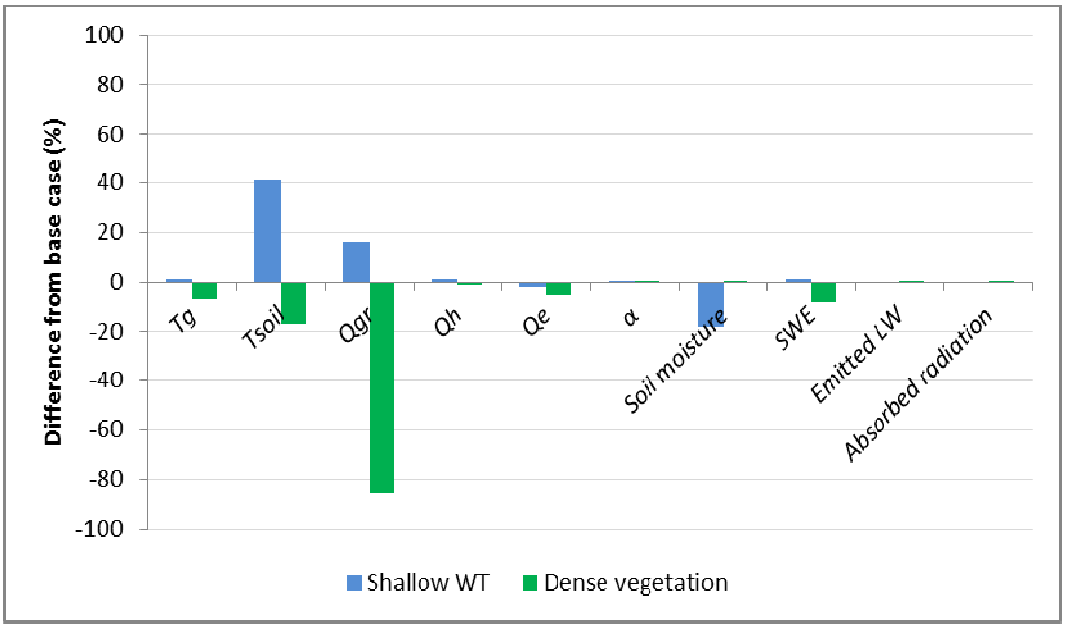

Fig. 7 Effects of dense vegetation and shallow water table.

Tg is ground temperature, *Tsoil* is soil temperature, *Qh* is sensible heat, *Qe* is latent heat, *α* is direct beam visible albedo, SWE is snow water equivalent, LW is long-wave radiation.

The effects of the shallow water table on the ground temperature and soil temperature are shown in Fig. 9. The shallow water table affects soil temperature (1.07°C higher than in the base case) and soil moisture content (larger than in the base case). Increased soil moisture results in two changes. First, it is less heat reflected from the ground. This is due to two factors—higher soil conductivity and lower albedo of saturated soils. Second, there is more evaporative (latent) heat because more water is available for evaporation. These changes have opposite effects—the first one increases soil temperature and the second one decreases soil temperature. The changes in ground heat are more important as evident from the temperature rise. The effects on the soil temperature are significant during the winter when the evaporation is low and soil temperature is 2.78°C higher. It is 0.51°C lower in the summer when the cooing from evaporation exceeds warming due to moist soil conditions.

As it is shown in Fig. 7, soil moisture (shallow water table) has noticeable impact on the soil temperature. The difference in the average annual soil temperatures is up to 2.0°C. The difference between the average monthly values is up to 6.4°C. However, its impacts on the ground temperatures are small. As a result, the short-term feedback to the atmospheric model is small as well.

While the short term effects of soil moisture are small, the long-term effects might be significantly larger. This is because the higher soil temperatures lead to greater thawing depths, which in turn may impact the permafrost condition and cause significant changes in the energy balance and feedback to the atmospheric model. These effects would take place over a significantly larger time scale than the simulation period of 100 years.

The effects of a shallow water table on the thawing depths are shown in Fig. 10. There are a number of years during which the thawing depth under the shallow water table condition is greater than in the base case. The years in which this depth increases to 0.83 m are the years in which the average soil temperature is at or above 0 in the shallow water table case while it is below 0°C in the base case.

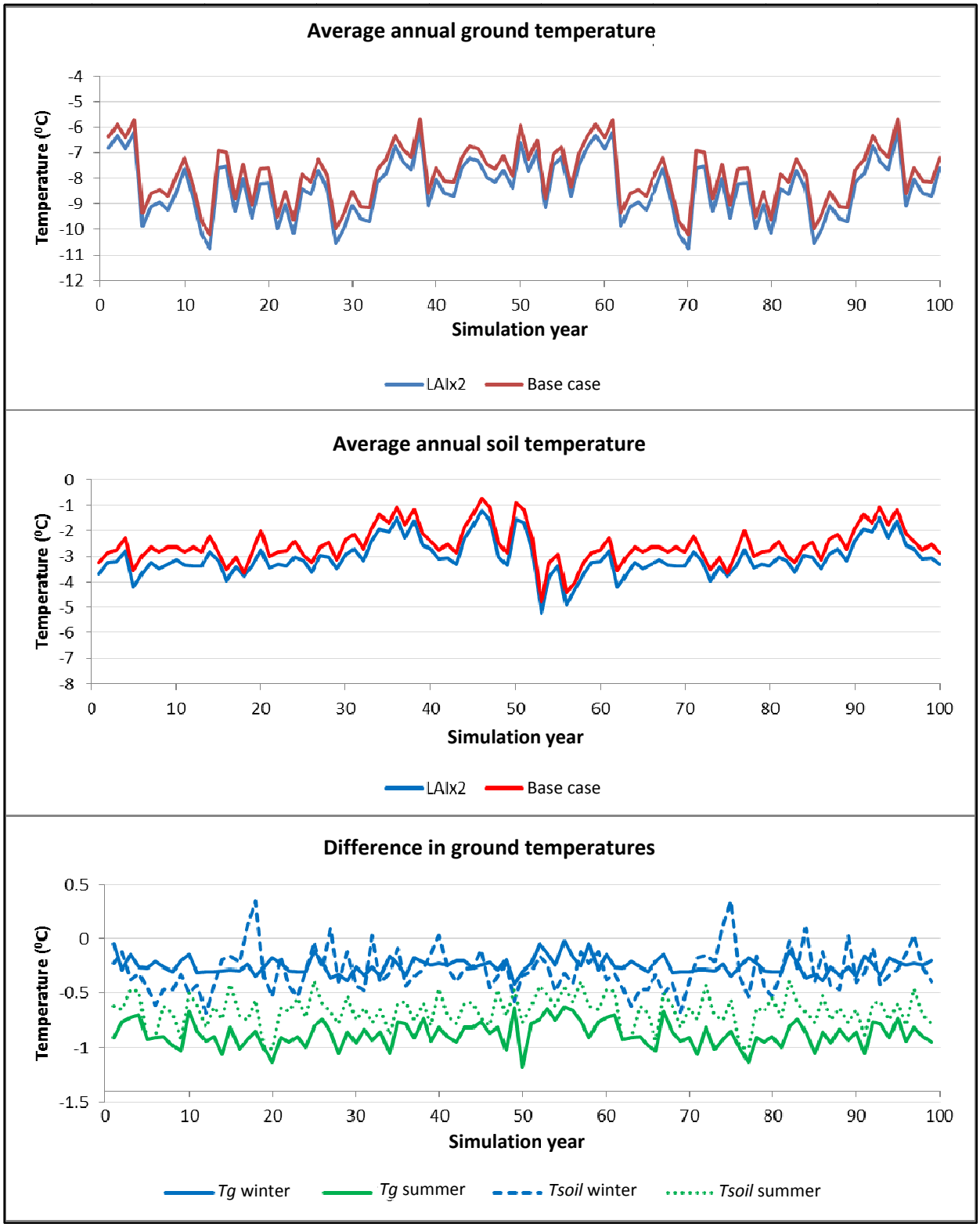

Fig. 8 Effects of dense vegetation on average annual and seasonal ground and soil temperatures.

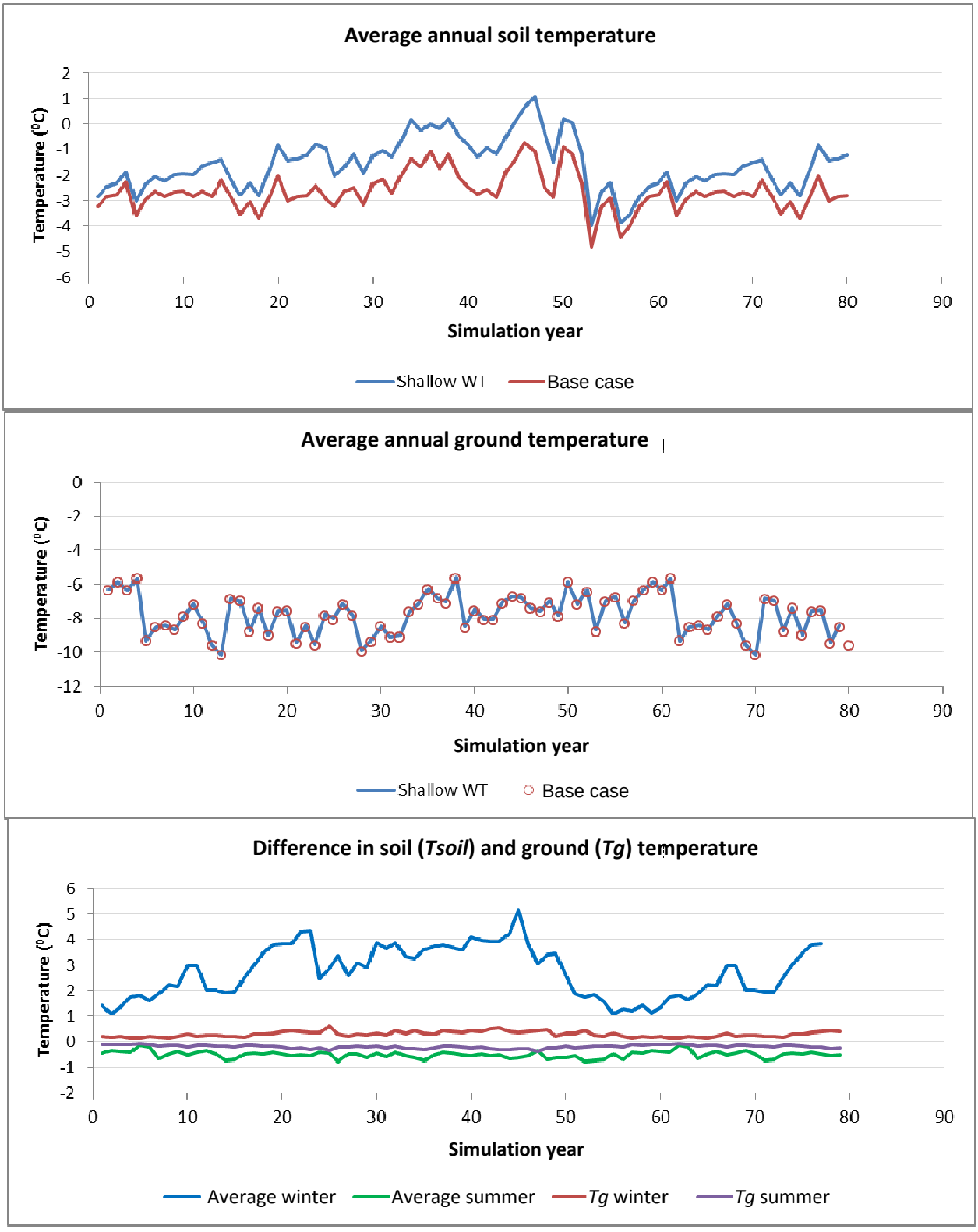

Fig. 9 Effects of shallow water table on average annual and seasonal ground and soil temperatures.

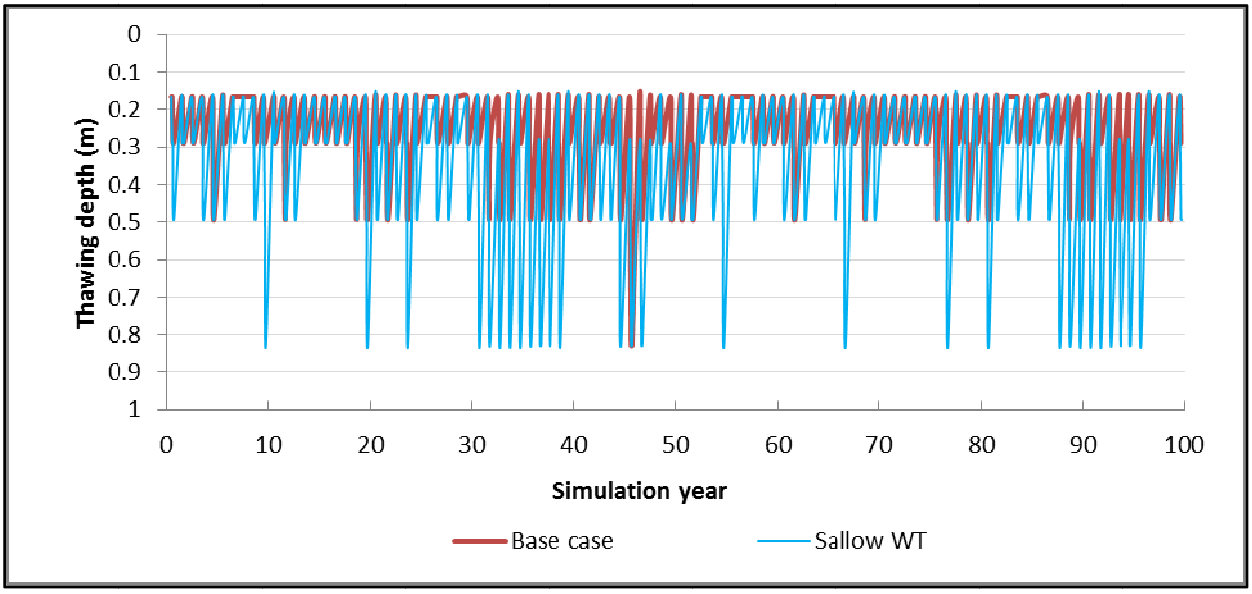

Fig. 10 Effects of shallow water table on thawing depth.

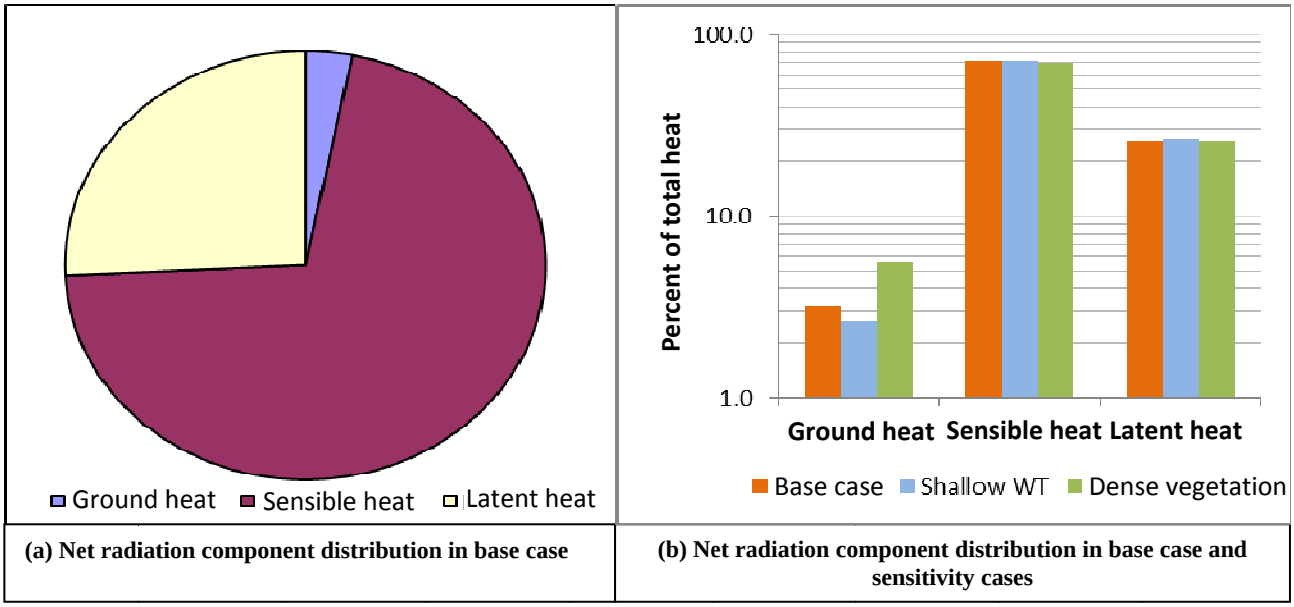

(a) Net radiation component distribution in base case

(b) Net radiation component distribution in base case and sensitivity cases

Fig. 11 Net radiation components comparison..

4. Discussion

The sensitivity analysis demonstrated that the only parameters that have a potential to impact the outputs are LAI, SAI, and shallow water table. The variations in the other parameters have negligible impacts.

These results can be explained based on the analysis of the net radiation (Q^*) partitioning at the land surface. The net radiation at the land surface (Q^*) is partitioned between the ground heat (Qg), sensible heat (Qh), and latent heat (Qe) as:

$$Q^* = Qg + Qe + Qh \quad (3)$$

The distribution of the net radiation components in the base case is shown in Fig. 11 (a). The sensible heat is the major component contributing 71.0% to the total. The latent heat is in the second place contributing 25.8%, and the ground heat has the smallest contribution of 3.2%.

Fig. 11 (b) provides a comparison between the different net radiation components obtained in the base

case and in the two sensitivity cases: shallow water table and maximum LAI (or dense vegetation). As it can be seen from this figure, the sensitivity cases have mostly impacted the ground heat. Because the ground heat is the smallest balance constituent in this environment, even noticeable changes in the ground heat have relatively small impact on the overall distribution of energy.

In case of the dense vegetation, the redistribution of energy is between the ground heat and sensible heat. In case of the shallow water table, the redistribution of energy is between the ground heat and latent heat.

5. Conclusions

The focus of this analysis was on the vegetation and soil models incorporated in CLM. Multiple CLM sensitivity runs were compared with regard to their effects on the feedbacks to the atmospheric model. The major conclusions of this analysis are:

The vegetation and soil parameters mostly affect the ground heat component of the energy balance, which in this environment is only about 3%. As a result, these parameters have relatively small impacts on the atmospheric inputs.

The most important parameters are the LAI and soil moisture. The other parameters have insignificant impacts on the energy distribution at the land surface.

The vegetation affects both, soil and ground temperatures, with the most impacts occurring during the summer when the LAI are at their maximum values.

The vegetation impacts ground temperature, which is highly correlated with the reference (atmospheric temperature). Because of this, the change in vegetation may impact the feedback into the atmospheric model and cause short-term changes in the climate.

The soil moisture noticeably increases soil temperature during the winter when the evaporation is low and slightly decreases temperature in the summer when evaporation is high.

Because soil temperature is weekly correlated with the ground temperature, the immediate impacts from the soil moisture are small. However, soil moisture may have significant long-term effects via its impacts on the depth of thawing.

The combined effects of soil moisture and vegetation are only slightly higher than the corresponding individual effects because the greatest impacts from vegetation are in the summer and greatest impacts from soil moisture are in the winter.

Acknowledgement

Sandia is a multi-program laboratory operated by Sandia Corporation, a Lockheed Martin Company for the United States Department of Energy's National Nuclear Security Administration under contract DE-AC04-94AL85000. The views expressed in this article are those of the authors and do not necessarily reflect the views or policies of the Department of Energy or Sandia National Laboratories.

References

[1] K.W. Oleson, D.M. Lawrence, G.B. Bonan, M.G. Flanner, E. Kluzek, S.L. Lawrence, et al., Technical Description of Version 4.0 of the CLM (Community Land Model), NCAR Technical Note NCAR/TN-478 + STR, Bolder, Colorado, 2010.

[2] T. Qian, A. Dai, K.E. Trenberth, K.W. Oleson, Simulation of global land surface conditions from 1948 to 2004, Part I: Forcing data and evaluations, Journal of Hydrometeorology 7 (5) (2006) 953-975.

[3] P.J. Lawrence, T.N. Chase, Representing a MODIS Consistent Land Surface in the Community Land Model (CLM 3.0), Part 1: Generating MODIS Consistent Land Surface Parameters, Technical report for Cooperative Institute for Research in Environmental Science, University of Colorado, Boulder, Colorado, 2006.

[4] C.A. Reynolds, T.J. Jackson, W.J. Rawls, Estimating available water content by linking the FAO Soil map of the world with global soil profile databases and pedotransfer functions, Water Resources Research 36 (12) (2000) 3653-3662.

[5] J. Diouf, Food and Agriculture Organization [CD-ROM], Digital Soil Map of the World, Rome, 1995.

[6] N.H. Batjes, A world data set of derived soil properties by FAOUNESCO soil unit for global modeling, Soil Use Management 13 (1) (1997) 9-16.

[7] R.B. Myneni, Global Products of vegetation leaf area and fraction absorbed par from year one of MODIS data,

Remote Sensing of Environment 83 (2002) 214-231.

[8] X. Zeng, M. Shaikh, A. Dai, R.E. Dickinson, R. Myneni, Coupling of the common land model to the NCAR community climate model, Journal Climate 15 (14) (2002) 1832-1854.

[9] X. Zeng, Global vegetation root distribution for land modeling, Journal of Hydrometeorology 2 (5) (2001) 525-530.

[10] S.D. Day, P.E. Wiseman, S.B. Dickinson, J.R. Harris, Contemporary concepts of root system architecture of urban trees, Arboriculture & Urban Forestry 36 (4) (2010) 149-159.